Fate of localization in a coupled free chain and a disordered chain

Xiaoshui Lin [1] and Ming Gong [1,2,3,*]

[1]*CAS Key Laboratory of Quantum Information, University of Science and Technology of China, Hefei 230026, China*

[2]*Synergetic Innovation Center of Quantum Information and Quantum Physics, University of Science and Technology of China, Hefei, Anhui 230026, China*

[3]*Hefei National Laboratory, University of Science and Technology of China, Hefei 230088, China*

(Received 17 August 2023; revised 22 January 2024; accepted 8 February 2024; published 15 March 2024)

It has been widely accepted that almost all states in one-dimensional disordered systems with short-range hopping and uncorrelated random potential are localized. Here, we consider the fate of these localized states by coupling between a disordered chain (with localized states) and a free chain (with extended states), showing that states in the overlapped and un-overlapped regimes exhibit totally different localization behaviors, which is not a localization-delocalization transition. In particular, while states in the overlapped regime are localized by resonant coupling, in the un-overlapped regime of the free chain the localization length is extremely large, which can be beyond the capability of state-of-art numerical methods, due to the prefactor t_v^4/Δ^4, where t_v is the interchain coupling strength and Δ is the band center offset between them. We confirm these results using the transfer-matrix method and sparse-matrix method for systems $L \approx 10^6$–10^9. These findings extend our understanding of localization in low-dimensional disordered systems and provide a concrete example, which may call for much more advanced numerical methods in high-dimensional models.

DOI: 10.1103/PhysRevA.109.033310

I. INTRODUCTION

Anderson localization (AL), which describes the phenomenon that the disorder totally suppresses the diffusion of the system, has attracted a great deal of attention for many decades [1–6]. It has been found that the spatial dimension plays an essential role in AL [7–11]. In the higher-dimensional models, a finite disorder strength is required for AL. However, in the one-dimensional (1D) tight-binding model with any weak random potential, almost all states are localized with spatial extension of the wave function as $|\psi(x)| \sim \exp[-|x - x_0|/\xi_0(E)]$, with E the corresponding energy. In a one-dimensional tight-binding model

$$H = -t \sum_i c_i^\dagger c_{i+1} + \text{H.c.} + \sum_i v_i c_i^\dagger c_i, \tag{1}$$

where t (assuming $t > 0$) is the hopping strength between the neighboring site, and v_i is the on-site random potential. The localization length is given by [12,13]

$$\xi_0^{-1}(E) = \frac{v^2}{8t^2 - 2E^2} = \frac{V^2}{96t^2 - 24E^2}, \tag{2}$$

where $v^2 = \langle v_i^2 \rangle$ is the variance of potential $v_i \in U(-V/2, V/2)$ (U denotes a uniform distribution) and E is the eigenvalue. The details of Eq. (2) can be seen from Eq. (14) in Ref. [12]. This result means that the states with the largest or lowest eigenvalues are more likely to be localized and that in the presence of any weak disorder, $0 < V \ll t$, with $|E| \leqslant 2t$, all states should be localized with $\xi_0^{-1} > 0$. For example, when $V \approx 0.1t$, $E = 0$, we have $\xi_0 \approx 10^4$, which can be directly confirmed by numerical simulation. The fate of the states in 1D systems will be changed fundamentally with incommensurate potentials [14–17], long-range correlated disorders [18–22], and many-body interactions [23–27], in which the localization-delocalization transition can be realized by tuning of disorder strengths. These physics have been intensively explored in experiments [28–31].

While the physics of disordered models have been widely discussed [3,9,13,32], the fate of localization by the coupling of extended and localized states is less investigated. We are interested in this issue due to the following dilemmas.

(i) The random uncorrelated potential induces localization for almost all states in 1D systems [8].

(ii) The hybridization between localized and extended states may lead to delocalization [33].

These two mechanisms lead to completely different physics, and their interplay should cause many intriguing phenomena. In this paper, we propose a coupled disordered model (Fig. 1) to address this problem. Our model is constructed from one free chain (with all states extended) and one disordered chain (with all states localized). This model can also be viewed as an alternative platform for the research of the localized insulator-bath problem. In the previous research, the bath is usually modeled as a k level quantum dot [34–36]. It is found that the bath can even induce a Zeno-like localization in the strong-coupling limit [34]. However, since the quantum dot does not have spatial structure, the feedback effect of the localized insulator on the bath has been neglected. In our model, we can investigate both the effect of the bath and the effect of the localized insulator, which support some different physics. Furthermore, our model is much more experimentally feasible and can be realized in ultracold atom gas with hyperfine structure [37] and an optical lattice with different

*gongm@ustc.edu.cn

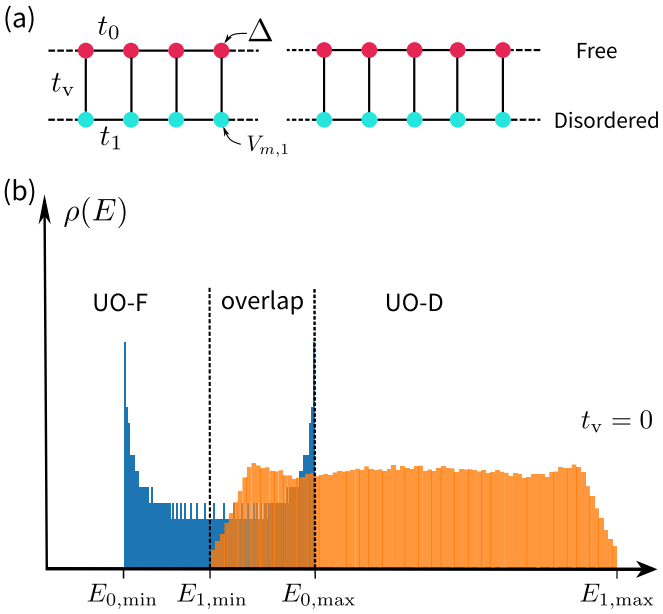

FIG. 1. (a) The realization of the coupled disordered model. The free chain (denoted as H_0) does not have random potential, thus all states are extended; yet in the disordered chain (denoted by H_1) with random potential, all states are localized. The coupling between them is the major concern of this paper. (b) The overlapped and un-overlapped spectra when $t_v = 0$, for eigenstates with $E_{1,\min} \leqslant E \leqslant E_{0,\max}$, with $E_{i,\max}$ and $E_{i,\min}$ being the maximal and minimal eigenvalues of H_i. $\rho(E) = \sum_i \delta(E - E_{i,\sigma})/L$ is the density of states for chain σ, with L the number of states. The value of $E_{1,\min}$ or $E_{1,\max}$ is determined numerically using $\rho(E_{1,\min})$, $\rho(E_{1,\max}) \approx 0.01 \max[\rho(E)]$. When $t_v \neq 0$ and weak, we can still use this definition for the overlapped and un-overlapped spectra approximately. In this paper, the un-overlapped regime from the free and disordered chains will be abbreviated as UO-F and UO-D, respectively.

disordered strengths [26]. Two major conclusions have been reached in this paper. First, we find that while all states exhibit localization in the presence of weak interchain coupling, their localization lengths exhibit distinct differences in the overlapped spectra and un-overlapped spectra. Secondly, the localization length for states in the un-overlapped regime from the free chain (UO-F) [see Fig. 1(b)] is given by

$$\xi^{-1}(E) \simeq \frac{t_v^4 V^2}{[96t^2 - 24(E-\Delta)^2]\Delta^4} = \frac{t_v^4}{\Delta^4}\xi_0^{-1}(E-\Delta), \quad (3)$$

in the limit when $|\Delta| \gg |V|$. Here, t_v is the interchain coupling, Δ is the band center offset between the free and disordered chains, and the argument $E - \Delta$ in ξ_0 is induced by the offset Δ between the two chains. This localization length can be much longer than the available system size in numerical calculation, exhibiting features resembling those in the extended phase. For instance, when $t_v = 0.1t$ and $\Delta = 10t$, the localization length can be $\xi \approx 10^8\xi_0$. We examine the above conclusions using the transfer-matrix method and the sparse-matrix method with system sizes $L \approx 10^6$–10^9. Our results show that the interchain coupling, disorder strength, and band center offset are the three major factors influencing the localization length of states in the UO-F regime. In the regime when $\xi \gtrsim L$, we can understand the localization of wave functions with the following general theorem based on a large amount of research; see review articles [3,9,38,39].

Theorem. In 1D disordered systems with short-range hopping and uncorrelated random potential, almost all states are localized in the thermodynamic limit ($L \to \infty$).

This theorem can be understood intuitively from the result by Mott and Twose [7], the argument by Thouless [40], and the scaling analysis by Abrahams *et al.* [8]. In the 1D disorder models, the β function is always negative for localization [8]. This theorem is also addressed by the celebrated Dorokhov-Mello-Pereyra-Kumar equation [38] and the nonlinear sigma model [41]. Here, not all states are localized because, in the 1D model with off-diagonal random hoppings, the state with $E = 0$ is extended while all the other states are localized [42]. Mathematicians have great interest in this problem and have proved this theorem with random potentials [43–46], showing no absolutely continuous spectra for extended states. This theorem will play a deterministic role for localization when $\xi \gtrsim L$, which is beyond the capability of the current numerical simulations.

The present paper is organized as follows. In Sec. II, we present the physical model and the numerical methods. In Sec. III, we discuss the different localization for states in the overlapped and un-overlapped spectra. In Sec. IV, a simple picture for understanding the localization in the un-overlapped spectra is discussed, and an analytical expression for its localization length is presented. In Sec. V, we summarize our primary conclusion and discuss the possible observations in experiments. Finally, in the Appendix, we present a discussion of the physics of the coupled disordered model in the strong-coupling limit.

II. PHYSICAL MODEL AND METHODS

We consider the following coupled disordered model (see Fig. 1):

$$\mathcal{H} = H_0 + H_1 + \sum_{m,\sigma} t_v a^\dagger_{m,\sigma} a_{m,\bar{\sigma}}, \quad (4)$$

where

$$H_0 = \sum_m t_0 a^\dagger_{m,0} a_{m+1,0} + \text{H.c.} + V_{m,0} a^\dagger_{m,0} a_{m,0}, \quad (5)$$

$$H_1 = \sum_m t_1 a^\dagger_{m,1} a_{m+1,1} + \text{H.c.} + V_{m,1} a^\dagger_{m,1} a_{m,1}, \quad (6)$$

with $\sigma = 0, 1$ [see Fig. 1(a)]. We set $V_{m,0} = \Delta$ for the offset of the free chain H_0 with $V_{m,1} \in U(-V/2, V/2)$ being the random potential for the disordered chain H_1. In the absence of interchain coupling (i.e., $t_v = 0$), the whole system can be decoupled into a free chain H_0 with all states extended, and a disordered chain H_1 with all states localized. Moreover, the energy spectra of each chain can be calculated individually with $E_{j,0} \in [E_{0,\min}, E_{0,\max}] = [-2t_0 + \Delta, 2t_0 + \Delta]$ for H_0 and $E_{j,1} \in [E_{1,\min}, E_{1,\max}]$ for H_1 [see Fig. 1(b)]. Thus, it is expected that these two energy spectra can be overlapped in the regime $[E_{1,\min}, E_{0,\max}]$, when $E_{0,\min} < E_{1,\max}$ and $E_{1,\min} < E_{0,\max}$, which can be realized when Δ is negative enough. Based on this, we define the three regimes as (1) UO-F, with $E \in [E_{0,\min}, E_{1,\min}]$; (2) the overlapped regime between both chains, with $E \in [E_{1,\min}, E_{0,\max}]$, if it exists; and (3) the

un-overlapped regime from the disordered chain (UO-D), with $E \in [E_{0,\max}, E_{1,\max}]$.

The notations of UO-F and UO-D are used in the figures for convenience. Then, if we switch on the interchain coupling ($t_\text{v} \neq 0$), assuming $|t_\text{v}| \ll t_\sigma$, the eigenstates of $\mathcal{H}$ would be the hybridization of the states from H_0 and H_1. We may expect all states to be exponentially localized due to the quasi-1D feature of the model. However, the localization behaviors should be different in the overlapped and un-overlapped spectra, which can be understood from the perturbation method. We term the zeroth-order states $|\psi^{(0)}_{j,\sigma}\rangle = |j,\sigma\rangle$ as

$$\left|\psi^{(0)}_{j,0}\right\rangle = \sum_m \frac{e^{ik_j m}}{\sqrt{L}} a^\dagger_{m,0}|0\rangle, \quad \left|\psi^{(0)}_{j,1}\right\rangle = \sum_m \phi(m) a^\dagger_{m,1}|m\rangle, \tag{7}$$

with $k_j = 2\pi j/L$, $\phi(m) \sim e^{-|m-m_j|/\xi}$. Then the new eigenstates at $t_\text{v} \neq 0$ can be written as

$$\left|\psi^{\text{new}}_{j,\sigma}\right\rangle = |j,\sigma\rangle + t_\text{v} \sum_i \frac{\langle i,\bar{\sigma}|H_\text{c}|j,\sigma\rangle}{E_{j,\sigma} - E_{i,\bar{\sigma}}}|i,\bar{\sigma}\rangle + \cdots, \tag{8}$$

with $H_c = \sum_{m,\sigma} a^\dagger_{m,\sigma} a_{m,\bar{\sigma}}$. Therefore, when $E_{j,\sigma}$ is in the overlapped spectra, the denominator for the first-order terms as well as the higher-order terms can be extremely small, yielding resonant hybridization. In contrast, this resonance would not happen when $E_{j,\sigma}$ is in the un-overlapped spectra. This indicates that the physics in the overlapped and overlapped spectra are rather different. It would be essential to characterize this difference during localization. When the coupling becomes much stronger than the other parameters, the concept of UO-F, UO-D, and overlapped is not well defined anymore. We have presented a discussion of this physics in the Appendix. In the main text, we focus on the weak-coupling limit.

We apply the transfer-matrix and sparse-matrix methods, whose available size is $L \approx 10^6$–10^9, to understand the localization of wave functions in these regimes. In the transfer-matrix method [47], the Lyapunov exponent $\gamma(E) = \xi(E)^{-1}$ is defined as the smallest positive eigenvalue of the matrix

$$\Gamma(E) = \lim_{L\to\infty} \frac{1}{2L} \ln(T_1^\dagger \ldots T_L^\dagger T_L \ldots T_1), \tag{9}$$

where T_m is the transfer matrix at the mth site. In our model, it is

$$T_m = \begin{pmatrix} \frac{E-\Delta}{t_0} & -\frac{t_\text{v}}{t_0} & -1 & 0 \\ -\frac{t_\text{v}}{t_1} & \frac{E-V_{1,m}}{t_1} & 0 & -1 \\ 1 & 0 & 0 & 0 \\ 0 & 1 & 0 & 0 \end{pmatrix}. \tag{10}$$

From the Oseledets ergodic theorem [48,49], the above multiplication of transfer matrices is converged when $L \to \infty$. When $\gamma(E) > 0$, the state with eigenvalue E is localized. In the sparse-matrix method, we use the shift-invert method [50,51] to obtain the eigenvalues and eigenvectors of $\mathcal{H}$. We first map $\mathcal{H}$ to

$$H_\text{shift-invert} = \frac{1}{E - \mathcal{H}}, \tag{11}$$

where E is the reference energy, and then perform the Lanczos method to calculate the eigenstates with the absolute value of the eigenvalues $|\lambda_i| = 1/|E - E_i|$ being the largest. We keep about $N_E = 20$ eigenstates $|\psi_{E_i}\rangle$ with eigenvalues E_i around the given E and perform 10^3–10^4 realization for the ensemble average. Furthermore, we characterize the structure of these wave functions using the averaged inverse participation ratio (IPR) as [3]

$$\langle \text{IPR}\rangle_E = \frac{1}{N_E} \sum_{i=1}^{N_E} \sum_{m=0}^{L-1} \sum_\sigma |\psi_{E_i}(m,\sigma)|^4. \tag{12}$$

For the extended state, $\langle \text{IPR}\rangle_E \propto L^{-1}$, and for the localized state $\langle \text{IPR}\rangle_E$ is finite. Finally, it is expected that $\langle \text{IPR}\rangle_E \sim L^{-D_2}$ when L is sufficiently large. Finally, we define the fractal dimension $D_2(E,L) = -d\ln(\langle \text{IPR}\rangle_E)/d\ln(L)$ and its limit $D_2(E) = \lim_{L\to\infty} D_2(E,L)$ to characterize their physics in the thermodynamic limit. We have $D_2(E) = 0$ for localized states, $D_2(E) = 1$ for extended states, and $0 < D_2(E) < 1$ for critical states [3,52,53]. We note that the IPR should be proportional to the Lyapunov exponent $\gamma(E)$ for an exponentially localized state $\psi_m \sim e^{-|m|/\xi}$, with IPR $\propto \xi^{-1} = \gamma$, in the limit $L \gg \xi$.

III. LOCALIZATION IN THE OVERLAPPED AND UN-OVERLAPPED REGIMES

Although all states are expected to be localized in our model in Eq. (4), the effect of interchain coupling for states in UO-F, overlapped, and UO-D regimes should be different, leading to distinct localization behavior. To have an intuitive picture of this difference, we consider two different cases, which are shown in Figs. 2(a) and 2(b). In the first case, the spectra in the two chains are largely separated to avoid the resonant hybridization between the extended and localized states, while in the second case resonant hybridization is induced in their overlapped regime. Furthermore, we present their typical wave functions in each energy regime in Figs. 2(c)–2(f) with $t_\text{v} = 0.1$, in which the wave functions in the component of H_0 are presented in Figs. 2(c) and 2(d), and those from H_1 are presented in Figs. 2(e) and 2(f). The results show that the wave functions in the UO-D regime are exponentially localized with localization length around unity (see the state with $E = 0$, $\xi \approx 1$). The wave functions in the overlapped regime are also exponentially localized [see $E = -5$ in Figs. 2(d) and 2(f)], however, with localization length $\xi \approx 10^4$, which is much larger than the localized states in the UO-D regime. Strikingly, the wave functions in the UO-F regime [see $E = -10$ in Figs. 2(c) and 2(e) and $E = -10$ in Figs. 2(d) and 2(f)] are extended even when the system size $L = 10^6$. Similar features can be found when L is increased to $L \approx 10^9$ for smaller t_v. These numerical evidences seem to contradict the general theorem. This dilemma is the major motivation for this paper.

To further characterize this dilemma, we use the IPR to describe the localization of wave functions quantitatively and study their scaling behaviors, with the results presented in Fig. 3. We obtain the eigenvalues using the shift-invert method for $L = 2^{11}$ to $2^{18} \approx 2.6 \times 10^6$. It is found that the IPR of states in the UO-D regime is around unity and does not change with the increasing of system size L, indicating localization.

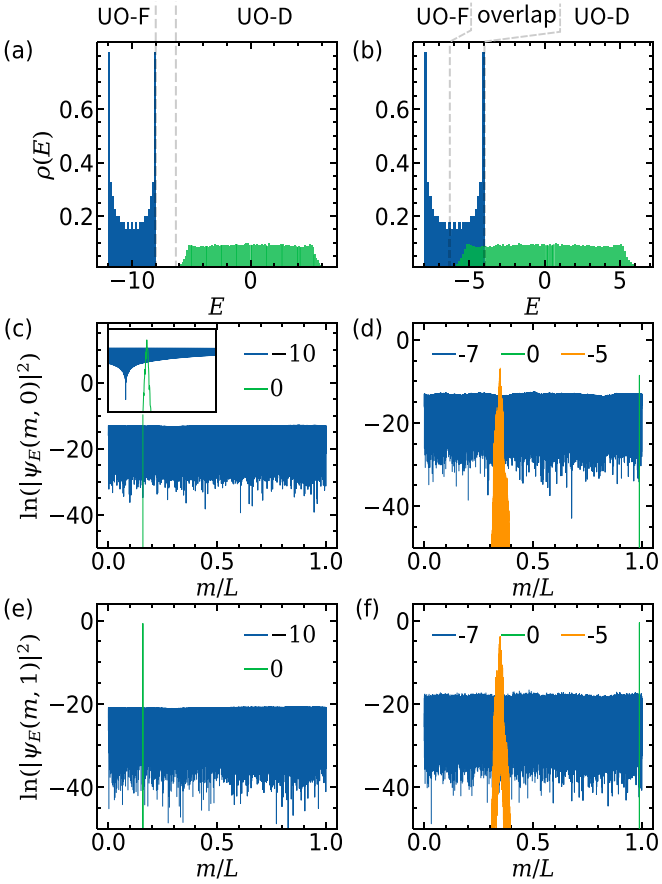

FIG. 2. [(a), (b)] The averaged density of states $\rho(E)$ for the free and disordered chains with $t_v = 0$. [(c), (d)] $\ln[|\psi_E(m,0)|^2]$ vs m with different E for the coupled disordered model ($t_v = 0.1$) in the first component $\sigma = 0$. The inset of (c) shows the detailed wave function around its localized center. [(e), (f)] $\ln(|\psi_E(m,1)|^2)$ vs m with different E for the coupled disordered model ($t_v = 0.1$) in the second component $\sigma = 1$. The parameters of the left column are $\Delta = -10$, $V = 10$, and $t_0 = t_1 = 1$, and those of the right column are $\Delta = -6$, $V = 10$, and $t_0 = t_1 = 1$. In (a) and (b) we use $L = 10^3$, and in (c)–(f) we use $L = 10^6$.

The value of the IPR for states in the overlapped regime [see Fig. 3(b)] is smaller than that in the UO-D regime, but we can still find that the IPR is saturated with the increase of system size L, indicating that the states in this energy regime are also localized with much larger localization length. However, we find the IPR of states in the UO-F regime exhibits features the same as that in the extended states. Especially, we find $\ln(\langle \mathrm{IPR}\rangle_E) = -\ln(L) + \mathcal{A}_E$, indicating these states to be extended even when the system size $L \approx 2^{18}$, which is consistent with the wave functions presented in Figs. 2(c)–2(f). This corresponds to the dilemma presented above, coming from the fact that $\xi \gg L \approx 10^5$, which is a finite-size effect. The localized behavior based on the general theorem can only be reached when $\xi \ll L$, which clarifies the disagreement presented in Fig. 2.

Next, we investigate the asymptotic behavior of the wave function using the transfer-matrix method, which can access the system with size $L \gg 2^{18}$. In Figs. 4(a) and 4(b), we present the Lyapunov exponent $\gamma(E)$ vs the energy E for

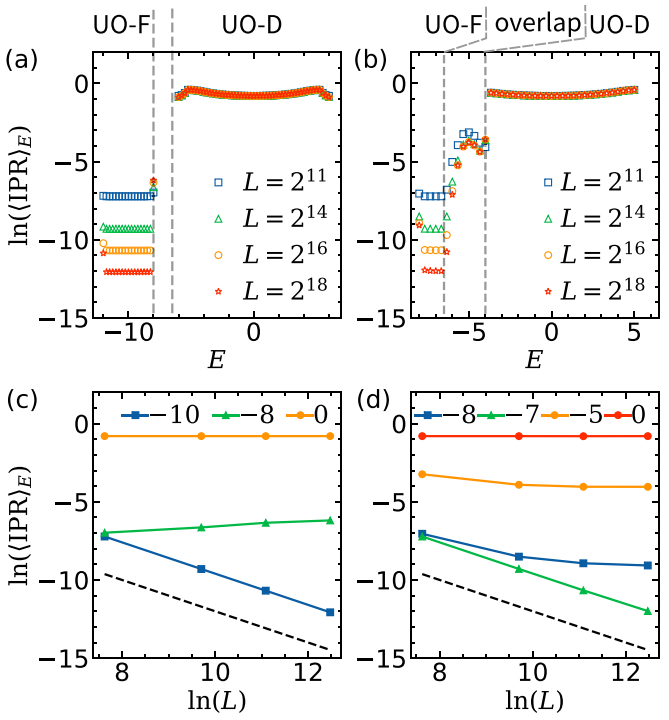

FIG. 3. [(a), (b)] ln(IPR) vs the energy E with (a) $\Delta = -10$, $V = 6$, and $t_0 = t_1 = 1$ and (b) $\Delta = -6$, $V = 6$, and $t_0 = t_1 = 1$ at different system sizes. The vertical dashed lines in (a) denote $E = -8$ and -6.4, and those in (b) denote $E = -6.4$ and -4. [(c), (d)] ln(IPR) vs $\ln(L)$ for states belonging to different energy regimes. The legends denote the corresponding energy. The parameters of (c) are the same as (a), and those of (d) are the same as (b). The slope of the black dashed lines is unity, which is a guide for the eye.

a system with size $L = 10^9$. When $t_v = 0$, the states in the free chain are extended and the states in the disordered chain are localized. When $t_v = 0.1$, all states become localized with $\gamma(E) > L^{-1}$. However, there are three distinct energy regimes for $\gamma(E)$, corresponding to the overlapped and un-overlapped regimes. In the overlapped regime, we have $\gamma(E) \approx 10^{-4}$, while in the un-overlapped regime, we have $\gamma(E) \approx 10^0$ (UO-D from the disordered chain) or $\gamma(E) \approx 10^{-7}$ (UO-F from the

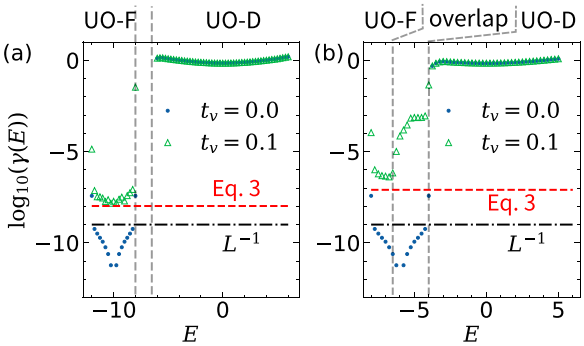

FIG. 4. The Lyapunov exponent $\gamma(E)$ vs the energy E for $t_v = 0$ and 0.1, with system size $L = 10^9$. The offset is (a) $\Delta = -10$ and (b) $\Delta = -6$. The vertical dashed lines in (a) denote $E = -8$ and -6.4, and those in (b) denote $E = -6.4$ and -4. The red dashed lines are estimated by Eq. (3).

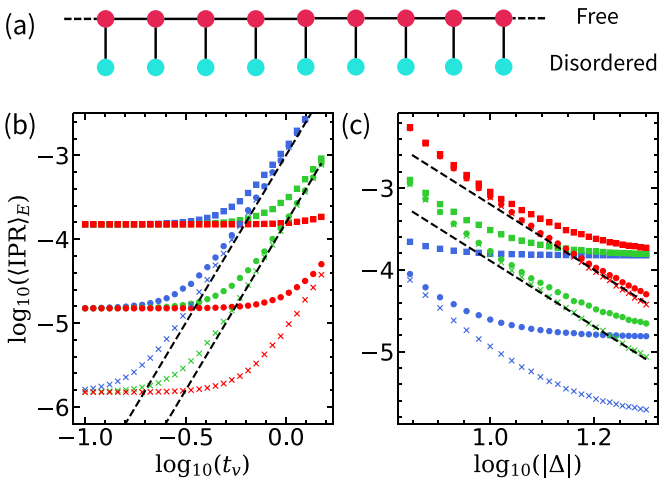

FIG. 5. (a) The schematic of the model in Eq. (13). The free chain H_0 (red) is coupled to a disordered chain H_1 (blue) with $t_1 = 0$. (b) $\log_{10}(\mathrm{IPR})$ vs $\log_{10}(t_v)$ for different band center offset Δ and lattice size L with $E = \Delta$. The colors represent $\Delta = -20$ (red), $\Delta = -10$ (green), and $\Delta = -7$ (blue). The system size is $L = 10^4$ (square), 10^5 (circular), and 10^6 (cross). The two black dashed lines are linear fittings with $\log_{10}(\langle \mathrm{IPR}\rangle_E) \approx 4\log_{10}(t_v)$. (c) $\log_{10}(\mathrm{IPR})$ vs $\log_{10}(|\Delta|)$ for different t_v. The meaning of symbols is the same as in (b). The colors represent $t_v = 1.5$ (red), $t_v = 1.0$ (green), and $t_v = 0.5$ (blue), and the black dashed lines denote $\log_{10}(\langle \mathrm{IPR}\rangle_E) \approx -4\log_{10}(|\Delta|)$.

the free chain). These distinct behaviors are unique features of the coupled disorder model, which should not be regarded as some kind of localization-delocalization transition. From the perturbation theory, these differences are rooted deeply in the resonant coupling and un-resonant coupling of wave functions, as discussed in Eq. (8).

IV. MECHANISM OF THE LOCALIZATION IN THE UN-OVERLAPPED REGIME

The above results raise some fundamental questions that need to be addressed much more carefully. In the overlapped regime, the localized states and extended states are coupled through resonant coupling because their energy is close to each other. From perturbation theory [see treatment in Ref. [1]; see Eq. (8)], all the higher-order terms will become important, leading to significant modification of the wave functions for localization. In the un-overlapped regime (regime UO-F) of the free chain, one also needs to consider all the higher-order terms for wave-function localization, yet with some different scattering processes. In the following, following the spirit of Thouless and Kirkpatrick [12] and Eq. (2), we derive a similar equation [see Eq. (3)] to describe the localization in the UO-F regime.

A. Analytical results with $t_1 = 0$

We first consider the limit with $t_1 = 0$ and $t_0 = 1$ (see Fig. 5), thus the Hamiltonian in Eq. (4) becomes

$$\mathcal{H} = H_0 + (t_v a^\dagger_{m,0} a_{m,1} + \mathrm{H.c.}) + V_{m,1} a^\dagger_{m,1} a_{m,1}. \quad (13)$$

As a consequence, the eigenstates of the disordered chain are fully localized at one site with the eigenvalue distributed in the interval $[-V/2, V/2]$ when $t_v = 0$. On the other hand, the eigenstates of the free chain are plane waves with energy spectra in $[\Delta - 2t_0, \Delta + 2t_0]$. It is expected that there will be no overlapped regime when $|\Delta| > |V/2 + 2t_0|$. We focus on the physics in this condition (with $t_v \neq 0$) for the characterization of the localization in the un-overlapped regime. This corresponds to the physics discussed in Fig. 2(a). The validity of this conclusion for the other conditions will be verified by numerical calculations in the next subsection.

In this case, we can eliminate the interchain coupling t_v and decouple the freedom of the free chain and disordered chain, which can be performed by the projection method. Then the effective Hamiltonian of each component reads as

$$H_{0,\mathrm{eff}} = \sum_m (t_0 a^\dagger_{m+1,0} a_{m,0} + \mathrm{H.c.}) + M_m a^\dagger_{m,0} a_{m,0}, \quad (14)$$

$$H_{1,\mathrm{eff}} = t_v^2 \sum_{m,n} G^{(0)}_{mn}(0) a^\dagger_{m,1} a_{n,1} + \sum_m V_{m,1} a^\dagger_{m,1} a_{m,1}, \quad (15)$$

with $M_m = \Delta + W_m = \Delta + t_v^2/(\Delta - V_{m,1})$ and $G^{(0)}_{mn}(E)$ the Green's function of H_0. For the free chain, we have

$$G^{(0)}_{mn}(E) = \langle m| \frac{1}{E - H_0} |n\rangle = \frac{1}{|t_0|\sqrt{x^2 - 4}} \left(\sqrt{\frac{x^2}{4} - 1} - \frac{|x|}{2} \right)^{|m-n|}, \quad (16)$$

with $|m\rangle = a^\dagger_{m,0}|0\rangle$ and $x = (E - \Delta)/t_0$. This result indicates that the disordered chain gains a hopping term with exponential decay between distance sites from the free chain, which increases the localization length. However, it could not drive a localization-delocalization transition from the general theorem. In contrast, the free chain gains a random potential term from the disordered chain, which in principle will immediately drive all states in the free chain to be localized even when $t_v^2 \ll t_0$. Hereafter we focus on the physics in $H_{0,\mathrm{eff}}$, in which M_m can be viewed as independently distributed random potential

$$\langle W_m \rangle = \frac{1}{V} \int_{-V/2}^{V/2} W_m dV_{m,1} = \frac{t_v^2}{V} \ln\left(\frac{2|\Delta| + V}{2|\Delta| - V} \right),$$
$$\langle W_m W_n \rangle = \frac{4t_v^4}{4\Delta^2 - V^2} \delta_{m,n}, \quad (17)$$

where $\langle\cdot\rangle$ represents its disorder averaged value, and $E \in [\Delta - 2t_0, \Delta + 2t_0]$. The variance of W_m can be written as

$$v^2 = \langle W_m^2 \rangle - \langle W_m \rangle^2 = t_v^4 \left(\frac{4}{4\Delta^2 - V^2} - f(\Delta, V) \right), \quad (18)$$

with

$$f(\Delta, V) = \left[\frac{1}{V} \ln\left(\frac{2|\Delta| + V}{2|\Delta| - V} \right) \right]^2. \quad (19)$$

Using the Thouless formula in Eq. (2), we can obtain

$$\xi^{-1}(E) = \left(\frac{4}{4\Delta^2 - V^2} - f(\Delta, V) \right) \frac{t_v^4}{8t_0^2 - 2(E - \Delta)^2}, \quad (20)$$

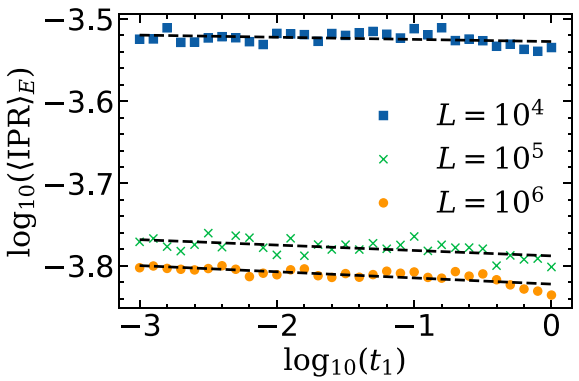

FIG. 6. $\log_{10}(\langle \mathrm{IPR}\rangle_E)$ vs $\log_{10}(t_1)$ for the model in Eq. (4) at different system sizes. The parameters are chosen as $\Delta = -10$, $t_v = 1$, and $E = -10$, corresponding to the UO-F regime. The black dashed lines are linear fittings with $\log_{10}(\langle \mathrm{IPR}\rangle_E) \sim \nu \log_{10}(t_1)$, with $\nu = -0.0026$ for $L = 10^4$, $\nu = -0.0066$ for $L = 10^5$, and $\nu = -0.0075$ for $L = 10^5$. Here, the wave functions are obtained using the shift-invert method around a given E.

with $E \in [\Delta - 2t_0, \Delta + 2t_0]$. When $\Delta \gg t_0$ and V, we can make use of Taylor expansion and it yields

$$v^2 = \frac{t_v^4 V^2}{12\Delta^4} + \frac{11 t_v^4 V^4}{360\Delta^6} + \mathcal{O}(\Delta^{-6}). \tag{21}$$

The leading terms give the localization length in Eq. (3), which is one of the central results in this paper and which has been used in Fig. 4. The coefficient in this expression will be slightly modified with a Gaussian distribution, with the major conclusion unchanged.

With this theoretical treatment, we next verify these results numerically. It should be noted that since the intrahopping t_1 of the disordered chain is set to zero, the transfer-matrix method cannot be employed [see Eq. (10), with T_m being singular]. Thus, we use the sparse-matrix method to examine the physics of the model in Eq. (13), and the results for states with $E = \Delta$ are presented in Fig. 5. It is found that $\langle \mathrm{IPR}\rangle_E \propto t_v^4$ at intermediate t_v and $\xi < L$. In the small t_v limit, we find the IPR will saturate to L^{-1} because $\xi \gtrsim L$. We expect the relation $\langle \mathrm{IPR}\rangle_E \propto t_v^4$ can be approached when $L \to \infty$. In Fig. 5(c), we also examine the dependence of IPR on the band center offset $|\Delta|$, finding that IPR $\propto \Delta^{-4}$ in the large $|\Delta|$ limit. However, when $t_v/|\Delta| \ll 1$ we have $\xi \gtrsim L$, and saturation of IPR is found again for the same reason as Fig. 5(b). Combining these two power-law dependences will yield $\xi^{-1} \propto (t_v/\Delta)^4$ in Eq. (3), using IPR $\propto 1/\xi$.

B. Applicability of the results to $t_1 \neq 0$

The previous conclusion is based on the model with $t_1 = 0$. However, our model in Eq. (4) has nonzero t_1. Thus, it is crucial to ask to what extent t_1 can influence the localization length ξ of the states in the free chain. To examine this effect, we fix $\Delta = -10$, $t_v = 1$, and $V = 10$ and change the value of t_1. The results of the IPR for states with $E \sim \Delta$ (belonging to the un-overlapped spectra of the free chain) are presented in Fig. 6, from which we find the IPR is nearly constant with the increasing of t_1, indicating that t_1 is not the essential term for the localization of the free chain. Therefore, we expect Eq. (3) to serve as a good approximation of localization length ξ even with finite t_1, which accounts for the excellent agreement between the numerical and theoretical results in Figs. 4(a) and 7. Finally, we present the relation between the localization length as a function of energy E in a single disordered chain and in a coupled disordered model in Fig. 7, which further confirms the empirical formulas of Eqs. (2) and (3).

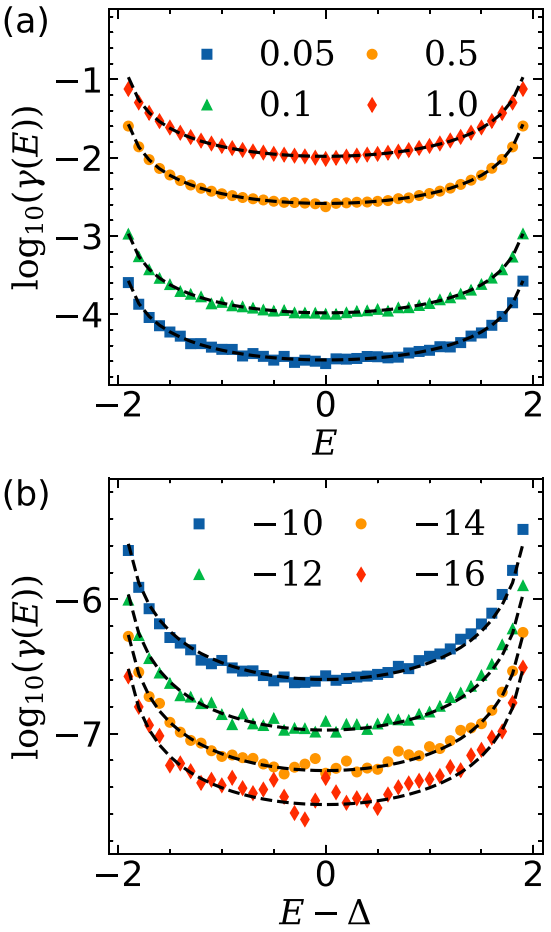

FIG. 7. The logarithm of the Lyapunov exponent $\gamma(E)$ vs the energy E. (a) Results for Eq. (1) with different disorder strengths V ($V = 0.05, 0.1, 0.5, 1.0$), with corresponding localization length by Eq. (2). (b) Results in the UO-F regime of the coupled disordered model in Eq. (4) with different band center offsets Δ ($\Delta = -16, -14, -12, -10$) with $t_0 = t_1 = 1$. The localization length is given by Eq. (20). In the transfer-matrix calculation, we have used $L = 2 \times 10^9$.

V. CONCLUSION AND DISCUSSION

In this paper, we present a coupled disordered model by coupling a disordered chain with a free chain, where the localization lengths in the overlapped and un-overlapped regimes differ by several orders of magnitude. In the overlapped regime, the states from the free chain are localized by resonant coupling between the localized and extended chains. However, in the UO-F regime, while the states are still localized by the general theorem, their localization lengths are much larger, due to the prefactor t_v^4/Δ^4. We find that the

interchain coupling, disorder strength, and band center offset play a leading role in localization, yet the effect of intrachain hopping t_1 in the disordered chain is not significant. The results presented in this paper are in 1D disordered models, and extending this research to higher-dimensional models [54–56] and many-body models [57–59] is also intriguing, in which we expect the overlapped regime and un-overlapped regime will also exhibit totally different behaviors [60]. Furthermore, for a system with a large localization length in the higher-dimensional models, it may call for much more advanced numerical methods.

These results can be readily confirmed in state-of-the-art experiments with ultracold atoms [5,61–64], in which the two chains can be realized by hyperfine states. The interchain coupling can be realized by Raman coupling and their band center offset is a natural consequence of detuning and Zeeman field. In these systems, the wave functions in each chain can be independently realized in the limit $t_v \approx 0$, and their localization can be measured individually using the time-of-flight imaging technique. In recent years, AL in disordered systems has been an important direction in ultracold atoms and huge progress has already been achieved [5,28,30,31,65–67], most of which have been focused on the physics of AL with incommensurate potentials and topological phase transitions with commensurate potentials. We expect our model can provide a platform for exploring wave-function localization, and the experimental confirmation of these results can provide perspicuous evidences for dilemmas I and II.

Finally, it is necessary to emphasize that the disordered potential (with short-range correlation) has totally different features from the incommensurate potential. In the coupled free chain and the incommensurate chain, without the guarantee of the general theorem, one can realize a critical phase in the overlapped spectra [53], in which the overlapped and un-overlapped spectra also exhibit distinct behaviors in localization. A similar critical phase by coupling of extended and localized states in the Floquet model with incommensurate potential has also been presented by Roy *et al.* in Ref. [68]. Here, we present a much-simplified model, which can be solved analytically in the limiting condition, in the hope that these intriguing results will be found in the more complicated coupled many-body models and coupled random matrices [69].

ACKNOWLEDGMENTS

This work is supported by the Strategic Priority Research Program of the Chinese Academy of Sciences (Grant No. XDB0500000) and the Innovation Program for Quantum Science and Technology (Grants No. 2021ZD0301200 and No. 2021ZD0301500).

APPENDIX: FATE OF LOCALIZATION IN THE PRESENCE OF STRONG COUPLING

For the sake of being self-contained, we present a discussion of physics in the limit of strong coupling, where the spectra are reconstructed. We still consider the Hamiltonian in Eq. (4) and set $t_0 = t_1 = t$, $V_{m,0} = M/4$, and $V_{m,1} = -M/4 + K_{m,1}$ with $K_{m,1}$ being random entries in $[-V/2, V/2]$. Using a local unitary transformation $c_m = \frac{1}{\sqrt{2}}(a_m + b_m)$ and

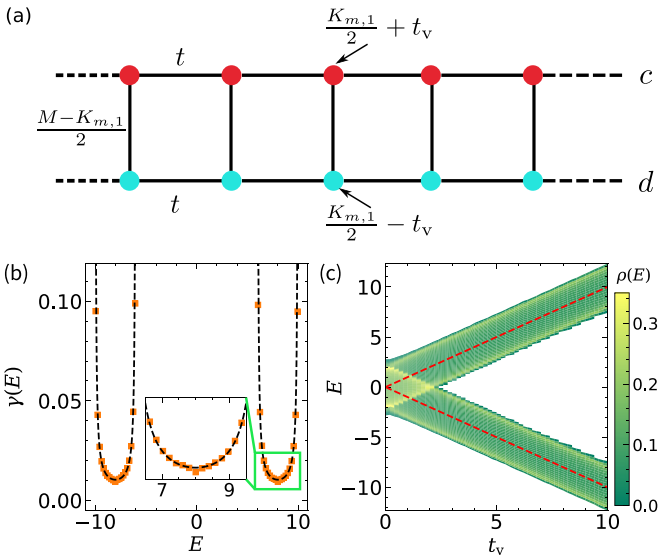

FIG. 8. (a) The schematic of the coupled chain via local transformation, in which the coupling t_v induces an energy offset in the c chain and d chain. (b) The Lyapunov exponent $\gamma(E)$ vs energy E in the coupled disordered model with $t_0 = t_1 = 1$, $M = 0$, $V = 2$, and $t_v = 20$. The square dots denote the numerical results and the dashed lines are the analytical results given by Eq. (A4). (c) Density of states $\rho(E)$ vs the coupling t_v and energy E. When t_v is large, the whole spectra are split into two bands. The red dashed lines denote $E = \pm t_v$.

$d_m = \frac{1}{\sqrt{2}}(a_m - b_m)$, we find the Hamiltonian becomes

$$\begin{aligned}\mathcal{H} = &\sum_m t(c_m^\dagger c_{m+1} + \text{H.c.}) + \left(\frac{K_{m,1}}{2} + t_v\right) c_m^\dagger c_m \\ &+ \sum_m t(d_m^\dagger d_{m+1} + \text{H.c.}) + \left(\frac{K_{m,1}}{2} - t_v\right) d_m^\dagger d_m \\ &+ \frac{M - K_{m,1}}{2}(c_m^\dagger d_m + d_m^\dagger c_m). \end{aligned} \tag{A1}$$

It was found that t_v becomes the offset of the c and d chains [see Figs. 8(a) and 8(c)]. We further require $|t_v| \gg |M|, |V| \gtrsim |t|$; thus, we can use the same treatment as in Sec. IV to decouple these two chains, from which we have

$$H_c = \sum_m t(c_m^\dagger c_{m+1} + \text{H.c.}) + \mathcal{W}_{m,c} c_m^\dagger c_m, \tag{A2}$$

$$H_d = \sum_m t(d_m^\dagger d_{m+1} + \text{H.c.}) + \mathcal{W}_{m,d} d_m^\dagger d_m, \tag{A3}$$

with $\mathcal{W}_{m,c} = \frac{K_{m,1}}{2} + t_v + \frac{(M-K_{m,1})^2}{8t_v - 2K_{m,1}}$ and $\mathcal{W}_{m,d} = \frac{K_{m,1}}{2} - t_v - \frac{(M-K_{m,1})^2}{8t_v + 2K_{m,1}}$. Here, we have neglected the effect of intrachain hopping t, which is too weak to be important. Using the Thouless formula and keeping the leading-order term of $1/t_v^2$, we find

$$\begin{aligned}\xi_\mu^{-1}(E) = &\frac{1}{8t^2 - 2(E \pm t_v)^2}\left[\frac{(M \pm 4t_v)^4 V^2}{12\,288 t_v^4}\right. \\ &\left. + \frac{11(M \pm 4t_v)^4 V^4}{5\,898\,240 t_v^6} + \mathcal{O}\left(\frac{1}{t_v^2}\right)\right], \end{aligned} \tag{A4}$$

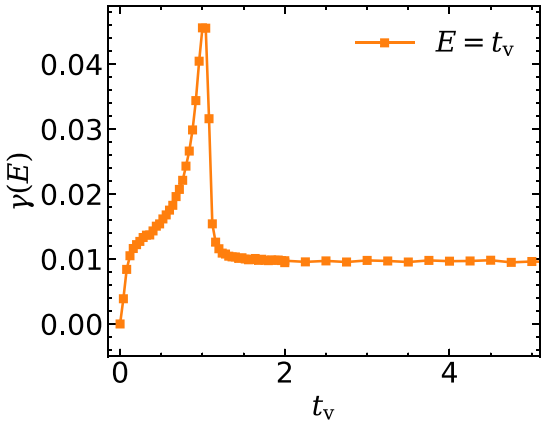

FIG. 9. Lyapunov exponent $\gamma(E)$ vs interchain coupling t_v for $E = t_v$. The energy corresponds to the red dashed lines in Fig. 8(c). Here, we use $L = 10^6$, $t = 1$, $V = 2$, and $M = 0$, which yields $\lim_{t_v\to\infty} \gamma(E = t_v) \approx 0.0104$.

with $\mu \in \{c, d\}$, and in $E \pm t_v$ and $M \pm 4t_v$ the minus sign is for c and the plus sign is for d. When $t_v \to \infty$, we find $\xi_\mu^{-1} \to \frac{V^2/4}{96t^2-24E^2}$, which is reduced to Eq. (2). A different possibility for the bath-localized insulator problem in a strong-coupling limit is discussed in Ref. [34]. We have also presented a numerical verification of this expression in Fig. 8(b), where excellent agreement between numerical and analytical results is achieved. Finally, we present the Lyapunov exponent as a function of interchain coupling t_v in Fig. 9. It is found that $\gamma(E)$ is a nonmonotonic function of t_v. When $t_v \ll 1$, the Lyapunov exponent in the overlap regime increases with the increasing of t_v. However, when $t_v \ll 1$, the overlap regime is not well defined and the Lyapunov exponent follows the prediction in Eq. (A4), which decreases with the increasing of t_v. The Lyapunov exponent exhibit a peak at about $t_v \approx 1$, which happens in the overlapped regime.

[1] P. W. Anderson, Absence of diffusion in certain random lattices, Phys. Rev. **109**, 1492 (1958).

[2] P. A. Lee and T. V. Ramakrishnan, Disordered electronic systems, Rev. Mod. Phys. **57**, 287 (1985).

[3] F. Evers and A. D. Mirlin, Anderson transitions, Rev. Mod. Phys. **80**, 1355 (2008).

[4] A. Lagendijk, B. van Tiggelen, and D. S. Wiersma, Fifty years of Anderson localization, Phys. Today **62**(8), 24 (2009).

[5] G. Roati, C. D'Errico, L. Fallani, M. Fattori, C. Fort, M. Zaccanti, G. Modugno, M. Modugno, and M. Inguscio, Anderson localization of a non-interacting Bose-Einstein condensate, Nature (London) **453**, 895 (2008).

[6] M. Segev, Y. Silberberg, and D. N. Christodoulides, Anderson localization of light, Nat. Photonics **7**, 197 (2013).

[7] N. F. Mott and W. D. Twose, The theory of impurity conduction, Adv. Phys. **10**, 107 (1961).

[8] E. Abrahams, P. W. Anderson, D. C. Licciardello, and T. V. Ramakrishnan, Scaling theory of localization: Absence of quantum diffusion in two dimensions, Phys. Rev. Lett. **42**, 673 (1979).

[9] K. Ishii, Localization of eigenstates and transport phenomena in the one-dimensional disordered system, Prog. Theor. Phys. Suppl. **53**, 77 (1973).

[10] D. J. Thouless, A relation between the density of states and range of localization for one dimensional random systems, J. Phys. C **5**, 77 (1972).

[11] D. J. Thouless, Localization distance and mean free path in one-dimensional disordered systems, J. Phys. C **6**, L49 (1973).

[12] D. J. Thouless and S. Kirkpatrick, Conductivity of the disordered linear chain, J. Phys. C **14**, 235 (1981).

[13] J. Heinrichs, Localization from conductance in few-channel disordered wires, Phys. Rev. B **66**, 155434 (2002).

[14] J. Biddle, B. Wang, D. J. Priour, and S. Das Sarma, Localization in one-dimensional incommensurate lattices beyond the Aubry-André model, Phys. Rev. A **80**, 021603(R) (2009).

[15] J. Biddle and S. Das Sarma, Predicted mobility edges in one-dimensional incommensurate optical lattices: An exactly solvable model of anderson localization, Phys. Rev. Lett. **104**, 070601 (2010).

[16] S. Ganeshan, J. H. Pixley, and S. Das Sarma, Nearest neighbor tight binding models with an exact mobility edge in one dimension, Phys. Rev. Lett. **114**, 146601 (2015).

[17] Y. Wang, X. Xia, L. Zhang, H. Yao, S. Chen, J. You, Q. Zhou, and X.-J. Liu, One-dimensional quasiperiodic mosaic lattice with exact mobility edges, Phys. Rev. Lett. **125**, 196604 (2020).

[18] F. M. Izrailev and A. A. Krokhin, Localization and the mobility edge in one-dimensional potentials with correlated disorder, Phys. Rev. Lett. **82**, 4062 (1999).

[19] F. A. B. F. de Moura and M. L. Lyra, Delocalization in the 1D Anderson model with long-range correlated disorder, Phys. Rev. Lett. **81**, 3735 (1998).

[20] O. Dietz, U. Kuhl, H.-J. Stöckmann, N. M. Makarov, and F. M. Izrailev, Microwave realization of quasi-one-dimensional systems with correlated disorder, Phys. Rev. B **83**, 134203 (2011).

[21] D. Delande and G. Orso, Mobility edge for cold atoms in laser speckle potentials, Phys. Rev. Lett. **113**, 060601 (2014).

[22] R. Johnston and B. Kramer, Localization in one dimensional correlated random potentials, Z. Phys. B **63**, 273 (1986).

[23] P. Bordia, H. P. Lüschen, S. S. Hodgman, M. Schreiber, I. Bloch, and U. Schneider, Coupling identical one-dimensional many-body localized systems, Phys. Rev. Lett. **116**, 140401 (2016).

[24] T. Thiery, F. Huveneers, M. Müller, and W. De Roeck, Many-body delocalization as a quantum avalanche, Phys. Rev. Lett. **121**, 140601 (2018).

[25] S.-H. Chiew, J. Gong, L.-C. Kwek, and C.-K. Lee, Stability and dynamics of many-body localized systems coupled to a small bath, Phys. Rev. B **107**, 224202 (2023).

[26] J. Léonard, S. Kim, M. Rispoli, A. Lukin, R. Schittko, J. Kwan, E. Demler, D. Sels, and M. Greiner, Probing the onset of quantum avalanches in a many-body localized system, Nat. Phys. **19**, 481 (2023).

[27] H. Ha, A. Morningstar, and D. A. Huse, Many-body resonances in the avalanche instability of many-body localization, Phys. Rev. Lett. **130**, 250405 (2023).

[28] D. H. White, T. A. Haase, D. J. Brown, M. D. Hoogerland, M. S. Najafabadi, J. L. Helm, C. Gies, D. Schumaye, and D. A. W. Hutchinson, Observation of two-dimensional Anderson localisation of ultracold atoms, Nat. Commun. **11**, 4942 (2020).

[29] H. P. Lüschen, S. Scherg, T. Kohlert, M. Schreiber, P. Bordia, X. Li, S. Das Sarma, and I. Bloch, Single-particle mobility edge in a one-dimensional quasiperiodic optical lattice, Phys. Rev. Lett. **120**, 160404 (2018).

[30] F. A. An, K. Padavić, E. J. Meier, S. Hegde, S. Ganeshan, J. H. Pixley, S. Vishveshwara, and B. Gadway, Interactions and mobility edges: Observing the generalized Aubry-André model, Phys. Rev. Lett. **126**, 040603 (2021).

[31] Y. Wang, J.-H. Zhang, Y. Li, J. Wu, W. Liu, F. Mei, Y. Hu, L. Xiao, J. Ma, C. Chin, and S. Jia, Observation of interaction-induced mobility edge in an atomic Aubry-André wire, Phys. Rev. Lett. **129**, 103401 (2022).

[32] P. W. Brouwer, C. Mudry, B. D. Simons, and A. Altland, Delocalization in coupled one-dimensional chains, Phys. Rev. Lett. **81**, 862 (1998).

[33] N. Mott, The mobility edge since 1967, J. Phys.: Condens. Matter **20**, 3075 (1987).

[34] D. A. Huse, R. Nandkishore, F. Pietracaprina, V. Ros, and A. Scardicchio, Localized systems coupled to small baths: From Anderson to Zeno, Phys. Rev. B **92**, 014203 (2015).

[35] D. Hetterich, M. Serbyn, F. Domínguez, F. Pollmann, and B. Trauzettel, Noninteracting central site model: Localization and logarithmic entanglement growth, Phys. Rev. B **96**, 104203 (2017).

[36] S. R. Koshkaki and M. H. Kolodrubetz, Inverted many-body mobility edge in a central qudit problem, Phys. Rev. B **105**, L060303 (2022).

[37] A. Rubio-Abadal, J. Y. Choi, J. Zeiher, S. Hollerith, J. Rui, I. Bloch, and C. Gross, Many-body delocalization in the presence of a quantum bath, Phys. Rev. X **9**, 041014 (2019).

[38] C. W. J. Beenakker, Random-matrix theory of quantum transport, Rev. Mod. Phys. **69**, 731 (1997).

[39] D. Belitz and T. R. Kirkpatrick, The Anderson-Mott transition, Rev. Mod. Phys. **66**, 261 (1994).

[40] D. J. Thouless, Electrons in disordered systems and the theory of localization, Phys. Rep. **13**, 93 (1974).

[41] K. B. Efetov, Supersymmetry and theory of disordered metals, Adv. Phys. **32**, 53 (1983).

[42] G. Theodorou and M. H. Cohen, Extended states in a one-dimensional system with off-diagonal disorder, Phys. Rev. B **13**, 4597 (1976).

[43] R. Carmona, A. Klein, and F. Martinelli, Anderson localization for Bernoulli and other singular potentials, Commun. Math. Phys. **108**, 41 (1987).

[44] H. Kunz and B. Souillard, Sur le spectre des opérateurs aux différences finies aléatoires, Commun. Math. Phys. **78**, 201 (1980).

[45] J. Fröhlich and T. Spencer, Absence of diffusion in the Anderson tight binding model for large disorder or low energy, Commun. Math. Phys. **88**, 151 (1983).

[46] L. A. Pastur, Spectral properties of disordered systems in the one-body approximation, Commun. Math. Phys. **75**, 179 (1980).

[47] *Computational Physics*, edited by Karl Heinz Hoffmann and Michael Schreiber (Springer-Verlag, Berlin, 1996).

[48] V. I. Oseledec, A multiplicative ergodic theorem: Lyapunov characteristic numbers for dynamical systems, Tr. Mosk. Mat. Obs. **19**, 179 (1968).

[49] M. S. Raghunathan, A proof of Oseledec's multiplicative ergodic theorem, Israel J. Math. **32**, 356 (1979).

[50] F. Pietracaprina, N. Macé, D. J. Luitz, and F. Alet, Shift-invert diagonalization of large many-body localizing spin chains, SciPost Phys. **5**, 045 (2018).

[51] D. J. Luitz, N. Laflorencie, and F. Alet, Many-body localization edge in the random-field Heisenberg chain, Phys. Rev. B **91**, 081103(R) (2015).

[52] H. Hiramoto and M. Kohmoto, Scaling analysis of quasiperiodic systems: Generalized Harper model, Phys. Rev. B **40**, 8225 (1989).

[53] X. Lin, X. Chen, G.-C. Guo, and M. Gong, General approach to the critical phase with coupled quasiperiodic chains, Phys. Rev. B **108**, 174206 (2023).

[54] E. Tarquini, G. Biroli, and M. Tarzia, Critical properties of the Anderson localization transition and the high-dimensional limit, Phys. Rev. B **95**, 094204 (2017).

[55] V. Janiš and J. Kolorenč, Mean-field theory of Anderson localization: Asymptotic solution in high spatial dimensions, Phys. Rev. B **71**, 033103 (2005).

[56] Y. Avishai and Y. Meir, New spin-orbit-induced universality class in the integer quantum Hall regime, Phys. Rev. Lett. **89**, 076602 (2002).

[57] R. Nandkishore and D. A. Huse, Many-body localization and thermalization in quantum statistical mechanics, Annu. Rev. Condens. Matter Phys. **6**, 15 (2015).

[58] F. Alet and N. Laflorencie, Many-body localization: An introduction and selected topics, C. R. Phys. **19**, 498 (2018).

[59] D. A. Abanin, E. Altman, I. Bloch, and M. Serbyn, *Colloquium:* Many-body localization, thermalization, and entanglement, Rev. Mod. Phys. **91**, 021001 (2019).

[60] X. Lin, M. Gong, and G.-C. Guo, From single-particle to many-body mobility edges and the fate of overlapped spectra in coupled disorder models, arXiv:2307.01638.

[61] C. Gross and I. Bloch, Quantum simulations with ultracold atoms in optical lattices, Science **357**, 995 (2017).

[62] N. D. Oppong, G. Pasqualetti, O. Bettermann, P. Zechmann, M. Knap, I. Bloch, and S. Fölling, Probing transport and slow relaxation in the mass-imbalanced Fermi-Hubbard model, Phys. Rev. X **12**, 031026 (2022).

[63] O. Mandel, M. Greiner, A. Widera, T. Rom, T. W. Hänsch, and I. Bloch, Coherent transport of neutral atoms in spin-dependent optical lattice potentials, Phys. Rev. Lett. **91**, 010407 (2003).

[64] B. Yang, H.-N. Dai, H. Sun, A. Reingruber, Z.-S. Yuan, and J.-W. Pan, Spin-dependent optical superlattice, Phys. Rev. A **96**, 011602(R) (2017).

[65] S. E. Skipetrov, A. Minguzzi, B. A. van Tiggelen, and B. Shapiro, Anderson localization of a Bose-Einstein condensate in a 3D random potential, Phys. Rev. Lett. **100**, 165301 (2008).

[66] T. Kohlert, S. Scherg, X. Li, H. P. Lüschen, S. Das Sarma, I. Bloch, and M. Aidelsburger, Observation of many-body localization in a one-dimensional system with a single-particle mobility edge, Phys. Rev. Lett. **122**, 170403 (2019).

[67] A. Dikopoltsev, S. Weidemann, M. Kremer, A. Steinfurth, H. H. Sheinfux, A. Szameit, and M. Segev, Observation of Anderson localization beyond the spectrum of the disorder, Sci. Adv. **8**, eabn7769 (2022).

[68] S. Roy, I. M. Khaymovich, A. Das, and R. Moessner, Multifractality without fine-tuning in a Floquet quasiperiodic chain, SciPost Phys. **4**, 025 (2018).

[69] X. Lin, G.-C. Guo, and M. Gong, Theory of mobility edge and non-ergodic extended phase in coupled random matrices, arXiv:2311.08643.